Roughening and preroughening in nonreconstructed fcc(110) surfaces: A Monte Carlo study

Giorgio Mazzeo
Institute for Theoretical Physics, University of Utrecht, TA 3508 Utrecht, The Netherlands and International School for Advanced Studies, via Beirut 4, 34014 Trieste, Italy

Giancarlo Jug
Dipartimento di Matematica e Fisica, Università di Camerino, 62032 Camerino, Italy and International School for Advanced Studies, via Beirut 4, 34014 Trieste, Italy

Andrea C. Levi
Dipartimento di Fisica, Università di Genova, via Dodecaneso 33, 16146 Genova, Italy

Erio Tosatti*
International School for Advanced Studies, via Beirut 4, 34014 Trieste, Italy
(Received 29 June 1993)

An anisotropic body-centered solid-on-solid (BCSOS) model Hamiltonian of the fcc(110) surface is reexamined and studied for the description of phase transitions on nonreconstructed noble- and near-noble-metal surfaces. The limit case corresponding to the isotropic BCSOS model is examined and some results are obtained for the staggered order-parameter susceptibility. With parameters roughly appropriate for a nonreconstructed surface such as Ag(110), a preroughening-type phase transition associated with the in-plane degrees of freedom is detected. It takes place somewhat below the roughening transition temperature and presents critical exponents which differ significantly from the two-dimensional Ising values. The analysis of the model is carried out through standard Monte Carlo simulation techniques. Scattering intensities are also evaluated, both to give a deeper insight into the disordered flat phase lying between the two transitions and to suggest a possible experimental verification of the proposed phase structure for the nonreconstructed two-sublattice surfaces.

I. INTRODUCTION

The topmost layer of the (110) surface of fcc crystal has an anisotropic structure which can be described in terms of atomic rows a distance a apart in the [001] direction (a being the fcc lattice parameter) and with the atoms separated by the close-packing distance $a/\sqrt{2}$ in the $[1\bar{1}0]$ direction (Fig. 1). This structure allows for the partitioning of the surface atoms into two separate, albeit equivalent, species ("black" B and "white" W), each associated with a distinct sublattice in the (110) plane, belonging to two distinct layers a distance $a_z = a/2\sqrt{2}$ apart (in the absence of relaxation). The two-sublattice structure introduces new possibilities for the thermal disordering of the atomic arrangement within the surface plane as well as outside this plane.

The fcc structure is, in particular, characteristic of the noble (Cu, Ag, and Au) and near-noble (Ni, Rh, Pd, Ir, and Pt) metals. The surface of the heavier fcc metals (e.g., Au and Pt) tends to increase its atomic density by means of the formation of (111) microfacets and the resulting structure is a more closely packed surface with lower surface energy. The lowest-order possibility of such microfaceting is the 2×1 missing-row reconstruction, where every second row is removed and the unit cell is doubled in the [001] direction.[1,2] On the other hand, most other fcc(110) metal surfaces (Ag, Cu, Ni, etc.) do not reconstruct, retaining at low temperature the original 1×1 structural symmetry. This work deals with the equilibrium structure of these nonreconstructed surfaces at temperatures $T>0$.

As temperature is increased, a number of disordering

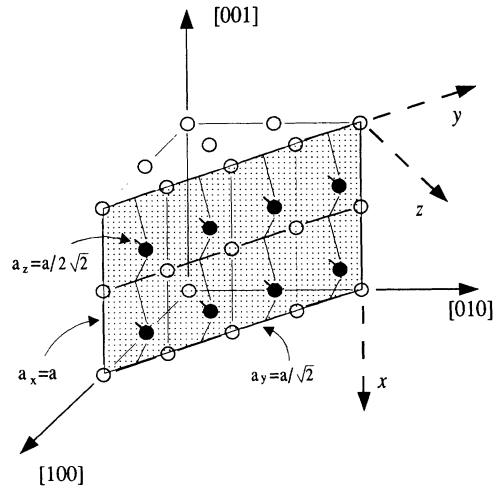

FIG. 1. The fcc lattice, cut so as to show the (110) surface, with the surface reference system x-y-z, the atomic spacings, and the two sublattices (black and white) in which the surface sites can be partitioned.

phenomena occur among the surface atoms. On the one hand, minor relaxation effects take place such as small lateral atomic displacements and inward relaxation of the top layers. More significantly, disordering collective phase changes occur at specific temperatures, involving either in-plane[1,2] or off-plane[3] order degrees of freedom, or both. Recently, there has been considerable interest in the structural phase transitions occurring on these fcc(110) metal surfaces, both from the experimental[4–15] and the theoretical[16–24] points of view. Much effort has been devoted to understanding the case of 2×1 reconstructing surfaces [Au(110) and Pt(110)], while less emphasis has so far been given to nonreconstructed ones [e.g., Ag(110), Cu(110), Ni(110), and, in another category, Pb(110)]. For reconstructing surfaces, an Ising-like in-plane disordering transition (deconstruction) has been detected[4,12–14] and the occurrence of roughening at a slightly higher temperature has also been demonstrated.[10,11]

Roughening[3] is characterized by a proliferation of steps due to the vanishing of the step free energy. Rommelse and den Nijs[16] have introduced the general concept of preroughening for low Miller index surfaces, where a disordered flat (DOF) phase, also characterized by a finite density of steps, occurs before out-of-plane roughening. In this paper we extend some of these ideas to the case of the fcc(110) surface and discuss the results of the Monte Carlo simulation of a model appropriate for a two-sublattice nonreconstructed structure such as Ag(110). This model was first proposed by our group for the study of reconstructed Au(110).[22]

We find that our model allows for two separate transitions to occur also for the nonreconstructed 1×1 surfaces.[24] Only in a limit case, corresponding to the well-known body-centered solid-on-solid (BCSOS) model,[25] we find that the two transitions coincide.[23] The lower-temperature transition, associated with the in-plane degrees of freedom, can always be ascribed to the recovery of full sublattice symmetry in the occupancy by atoms of the two species (B and W) of the topmost surface layer. Within our approach, we believe that this transition manifests itself in terms of the two-dimensional Ising deconstruction in the case of the 2×1 reconstructed surfaces, while it takes the form of variable exponents preroughening for the nonreconstructed 1×1 case. In either case the higher-temperature transition involves the off-plane degrees of freedom (local interfacial heights) and takes the form of a standard Kosterlitz-Thouless-type roughening,[3] irrespective of the two-sublattice underlying surface structure.

It is notable that all these transitions can be described by one and the same model, which therefore accounts for the complete interplay between in-plane ordering and roughening in fcc(110) surfaces. Indeed, the very same monoatomic surface steps that account for the roughening of these surfaces are also responsible, when bound by energy or entropy constraints, for the destruction of the in-plane ordering. A parallel description, due to den Nijs,[17] of this interplay already exists in the literature, where a related model is proposed for the reconstructing fcc(110) surfaces. It is therefore worth presenting in this paper the details of the calculations carried out on our model for the nonreconstructed fcc(110) surfaces. Beside the information on phase transitions, our work also affords some knowledge on the nature of the intermediate DOF phase through the evaluation of scattering correlation functions. We stress that the model's parameters chosen to represent the case of Ag(110) have been taken so as to agree roughly with first-principle many-body calculations for these systems.[26] Therefore our study also allows for the important comparison with experimental data for the conclusions drawn from our analysis.

The remainder of the paper is organized as follows. In Sec. II we repropose our model and discuss the low-temperature surface structures it can describe. General ground-state considerations are given and the relevant physical quantities suitable for simulation and experimental analysis are introduced. Particular attention is paid to the *order parameters* accounting for the phase transitions to be described and to the presentation of the scattering functions. In Sec. III a limit case of our Hamiltonian, corresponding to the BCSOS model, is considered to test our Monte Carlo simulation procedure, both in reproducing exact known properties and in predicting the behavior of relevant physical quantities such as the staggered, or sublattice, order parameter and its susceptibility. In Sec. IV the simulation is carried out for the Ag(110) system, with the prediction of a sublattice disordering (or preroughening) phase transition and with its characterization in terms of critical exponents. Finally, Sec. V contains our conclusions. Preliminary accounts for some of the results presented below have been presented elsewhere.[23,24]

II. THE MODEL AND THE RELEVANT PHYSICAL QUANTITIES

Collective surface disordering phenomena are often studied within solid-on-solid (SOS) models, particularly inasmuch as the off-plane degrees of freedom and roughening are concerned. Relaxation effects do take place in the first few atomic layers of the surface; however, it is generally believed that a description in terms of atomic columns still holds good for the study of the roughening and other lower-temperature transitions. Our model for the fcc(110) metal surfaces[22] makes use of an anisotropic SOS Hamiltonian defined on a lattice

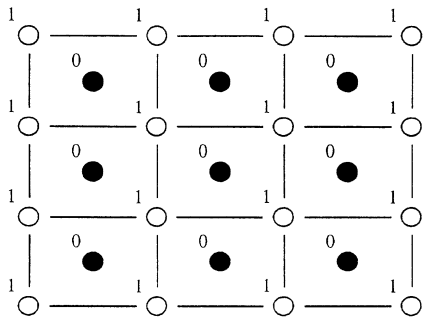

FIG. 2. A schematic representation of the B and W sublattices on which our SOS model is defined. Also indicated are the heights corresponding to the nonreconstructed ground state.

made up of two (B and W) interpenetrating rectangular sublattices on which sites the column height integer variables h_i are assigned for each configuration. We choose to assign even integers to the B sites and odd ones to the W sites. Neighboring columns' height jumps are restricted to be ± 1 in our (restricted SOS) model. Figure 2 shows the B and W sublattices, with explicit indication of the heights corresponding to the 1×1 ground state. With reference to Fig. 3, the Hamiltonian reads

$$\begin{aligned}\mathcal{H}/J=&\sum_i [h(\mathbf{r}_i)-h(\mathbf{r}_i+\hat{\mathbf{y}})]^2 \\ &-K_2\sum_i [h(\mathbf{r}_i)-h(\mathbf{r}_i+\hat{\mathbf{x}})]^2 \\ &+\tfrac{1}{2}K_3\left[\sum_i [h(\mathbf{r}_i)-h(\mathbf{r}_i+\tfrac{3}{2}\hat{\mathbf{x}}+\tfrac{1}{2}\hat{\mathbf{y}})]^2\right. \\ &\left.+\sum_i [h(\mathbf{r}_i)-h(\mathbf{r}_i+\tfrac{3}{2}\hat{\mathbf{x}}-\tfrac{1}{2}\hat{\mathbf{y}})]^2\right] . \qquad (2.1)\end{aligned}$$

Here $\hat{\mathbf{x}}$ and $\hat{\mathbf{y}}$ are the single rectangular sublattice unit vectors in the [001] and [1$\bar{1}$0] directions. J measures the atomic cohesion energy and K_2J and K_3J are second-neighbor and third-neighbor couplings simulating the effect of long-ranged interaction potentials. Each of the terms contained in the Hamiltonian assigns an energy cost (or gain) to neighboring pairs of sites that are found at height differences greater than 0 (same sublattice) or 1 (different sublattices). The first term thus encourages the formation of long atomic rows in the y direction. The K_2 term serves the same purpose in the x direction, if negative; when $K_2>0$, it encourages the surface profile to descend or rise and attain a (111) facet configuration. In order to recover a 2×1 reconstructed configuration the K_3 term has to be included in the Hamiltonian, with $K_3>0$. This last term would seem not so important for a nonreconstructed ground state. However, the tendency to reconstruct is dormant in all these surfaces and an energy term which mimics the long-range many-body interactions of the real surfaces has nonetheless to be used in order to reproduce the correct physics. It is now easy to see, by evaluating the energies of specific surface configurations (see below), that the relevant interaction parameter at $T=0$ is $\kappa=K_2/K_3$, in terms of which the ground-state phase diagram is as follows:

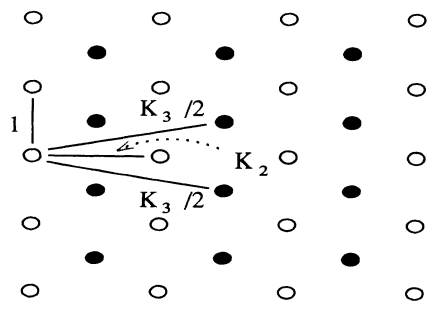

FIG. 3. The structure of the couplings between sites in our model. The parameters are expressed in units of J.

$$\begin{aligned}&\kappa<0 \quad [1\times 1 \text{ nonreconstructed (110)}] , \\ &0<\kappa<4 \quad [2\times 1 \text{ reconstructed (110)}] , \\ &\kappa>4 \quad [(111) \text{ faceting}] .\end{aligned} \qquad (2.2)$$

Thus, for $\kappa>4$ the surface facets into a macroscopic (111) surface: this effect, however, is not observed in any known metal. We remark that this model is equivalent to one of the models (model I) proposed by Levi and Touzani.[28]

It is important also to notice that in the limit $\kappa\to-\infty$, i.e., $K_3\to 0$ with $K_2<0$, the above Hamiltonian becomes the same as that appropriate for the anisotropic version of the BCSOS model.[20,29] Since this model affords some rigorous exact results for its thermodynamics, it will be used below as a limit case in order to test our simulation procedure, as well as to understand the statistical properties of the full model.

In order to fix the parameters J, K_2, and K_3 so as to describe a specific fcc(110) metal surface, it is appropriate to compare the expressions we obtain from Hamiltonian (2.1) for the energies of certain surface configurations to the values available from either embedded-atom[26] or glue-model[27] calculations. Experimental values of the surface energies cannot be used for this purpose, as they refer either to average values over surfaces of polycrystalline samples or, in most favorable cases, to room-temperature surface free energies, where entropy effects cannot be ignored. The general expressions for the $T=0$ energies of the (110) surface and for its $n\times 1$ reconstructions are, from Eq. (2.1),

$$\begin{aligned}&E_{1\times 1}/J\mathcal{N}=K_3 , \\ &E_{n\times 1}/J\mathcal{N}=-4\frac{n-1}{n}K_2+\frac{9n-16}{n}K_3 \quad (n=2,3,\ldots,\infty) , \\ &E_{100}/J\mathcal{N}=4+K_3 ,\end{aligned} \qquad (2.3)$$

apart from a constant contribution E_0, and where we have also displayed the expression for the energy of the (100) face.

Fitting these expressions to the results of Ref. 27 has already allowed for the simulation of the Au(110) system. For Ag, which is taken in this work as the representative element of the group of nonreconstructed noble and near-noble metals (ignoring, however, specific complications that Ag itself may present[6]), we extract the model parameters from the data obtained by Chen and Voter[26] through the embedded atom method. Actually, the available embedded-atom method results yield values for the energies of several surface configurations. The set of data is therefore overcomplete; however, by a reasonable interpolation of these data we extract the following parameters:

$$\begin{aligned}&E_0\simeq 350 \text{ meV}, \quad J\simeq 34 \text{ meV}\simeq 400 \text{ K} , \\ &K_2\simeq -0.1, \quad K_3\simeq 0.025 ,\end{aligned} \qquad (2.4)$$

with which $\kappa=K_2/K_3$ is negative, $\kappa=-4.0$, in agreement with the nonreconstructed nature of Ag(110).

Many continuous phase transitions are characterized

by the vanishing of a suitable order parameter. We consider in this work the order parameters characterizing preroughening and sublattice disordering. According to Rommelse and den Nijs,[16] within a restricted solid-on-solid model of the sc(100) face the column parity variable $\sigma_i = \exp[i\pi h(\mathbf{r}_i)] = \pm 1$ defines a local quantity which changes sign every time an up or down step occurs in a given configuration. This variable averages out to zero when a finite density of steps develops on the surface, even though the surface remains flat; for a flat surface in the absence of steps, however, $\langle \sigma_i \rangle = \rho \neq 0$ denotes a phase with a broken symmetry in the parity. An order parameter for the preroughening transition can still be conveniently defined for an fcc(110) surface, provided the following modifications are introduced. The local step-sensitive variable, e.g., for a site $\mathbf{r}_i$ belonging to the B sublattice, will be defined as

$$\sigma_i^B = \tfrac{1}{4} \sum_{\delta} [h(\mathbf{r}_i) - h(\mathbf{r}_i + \delta)] , \tag{2.5}$$

where the sum is over the four neighboring W sublattice sites. This variable takes five possible values: $+1$, $+\frac{1}{2}$, 0, $-\frac{1}{2}$, and -1, although below roughening the predominant values will be just $+1$ and -1 if σ_i^B is coarsened over a few lattice spacings. At $T=0$ the average

$$\rho = \langle \sigma_i^B \rangle \tag{2.6}$$

equals $+1$ or, equivalently, -1, while as steps and terraces develop on the surface at $T>0$ the absolute value of ρ decreases until it vanishes at the preroughening temperature T_{PR} where an up-down ordered (but randomly spaced) structure of steps develops on the surface. Indeed, σ_i^B changes sign every time a monoatomic step occurs in any given direction. ρ is therefore the *preroughening order parameter* appropriate for a two-sublattice surface structure such as fcc(110).

Alternatively, we could introduce another crucial physical quantity, which we may call the *sublattice order parameter,* which takes the value $+1$ (or -1) at $T=0$ when either the B or W sublattice atoms describe the top surface layer and the value 0 above a characteristic temperature $T_{B/W}$ when no sublattice type prevails in the top layer. This second order parameter is thus sensitive to the symmetry between the given sublattices in describing the surface profile, a symmetry which gets spontaneously broken at low temperatures in respect of the degeneracy between the ground states. The symmetry is recovered above $T_{B/W}$; we point out that we expect $T_{B/W} \leq T_R$ since sublattice disordering is still concerned with in-plane degrees of freedom. A natural definition for the sublattice order parameter of an fcc(110) [or bcc(100)] two-sublattice surface is as follows.[30] Define the composite probabilities of choosing, say, a B site atom and stepping up from it, P_B^+, and that of stepping down, P_B^-, to one of its four W nearest neighbors ($P_B^+ + P_B^- = \frac{1}{2}$) through

$$P_B^- = \sum_{\text{even } h=-\infty}^{+\infty} p(h) b(h) , \tag{2.7}$$

where the sum extends over all even B site heights h and the analogous definition holds for P_W^- with a sum running over all odd heights. The above definition is general, but particularly useful for the BCSOS model for which exact expressions for $p(h)$, the probability of finding a surface atom at height h, and $b(h)$, the probability of stepping down from an atom at height h, can be derived (see Sec. III). Alternatively, P_B^- can be viewed as the statistical average of a local probability[23]

$$\begin{aligned} P_B^- &= \langle p_B^-(\mathbf{r}_i) \rangle , \\ p_B^-(\mathbf{r}_i) &= \tfrac{1}{4} \left[1 + h(\mathbf{r}_i) - \tfrac{1}{4} \sum_{\delta} h(\mathbf{r}_i + \delta) \right] , \end{aligned} \tag{2.8}$$

taking the values $\frac{1}{2}$, $\frac{3}{8}$, $\frac{1}{4}$, $\frac{1}{8}$, and 0 for the five distinct configurations of the four W neighbors of a B atom. The analogous definition holds for $p_B^+(\mathbf{r}_i)$ and leads to $p_B^-(\mathbf{r}_i) + p_B^+(\mathbf{r}_i) = \frac{1}{2}$. We then define the order parameter as

$$P_{B/W} = \frac{P_B^- - P_W^-}{P_B^- + P_W^-} , \tag{2.9}$$

which clearly takes the value $+1$ (or -1) in the ground state and 0 in the sublattice disordered phase. Since for the BCSOS topology we also have $P_B^- + P_W^- = \frac{1}{2}$, we obtain

$$P_{B/W} = 4P_B^- - 1 . \tag{2.10}$$

For a finite system, we average both over all configurations and lattice sites to get

$$P_{B/W} = \frac{2}{\mathcal{N}} \left\langle \sum_B h_B - \sum_W h_W \right\rangle , \tag{2.11}$$

where the limit $\mathcal{N} \to \infty$ is understood for a proper definition of the order parameter ($\mathcal{N}$ is the combined total number of B and W sites). $T_{B/W}$ is therefore the sublattice disordering temperature above which the B and W site atoms populate the surface topmost positions with equal probability. Although for the two-sublattice surfaces at hand the in-plane phase transition can be more appropriately termed *sublattice disordering,* it is not difficult to show that the order parameters ρ and $P_{B/W}$ are one and the same quantity. Indeed, a global representation of ρ takes the form

$$\begin{aligned} \rho &= \frac{2}{\mathcal{N}} \left\langle \sum_{i \in B} \sigma_i^B \right\rangle \\ &= \frac{1}{2\mathcal{N}} \left\langle \sum_{\delta} \sum_{i \in B} [h(\mathbf{r}_i) - h(\mathbf{r}_i + \delta)] \right\rangle \\ &= P_{B/W} , \end{aligned} \tag{2.12}$$

so that the sublattice disordering transition is just the same as preroughening. A similar conclusion can be reached for 2×1 reconstructed systems (see the Appendix).

In order to investigate the thermodynamic properties of our fcc(110) surface, a standard Monte Carlo technique is applied to a lattice of $\mathcal{N} = 2 \times N_x \times N_y$ sites, with $N = N_x = N_y = 12$, 16, 20, 24, 28, and 32, and with periodic boundary conditions. We have evaluated the order pa-

rameter $P_{B/W}$ defined through Eq. (2.11), where the absolute value is taken before statistical averaging in order to ensure a meaningful procedure. Fluctuations in the order parameter $P_{B/W}=\langle \mathcal{P}_{B/W} \rangle$ have been investigated through the related susceptibility

$$\chi_{B/W}=\frac{\mathcal{N}}{2k_BT}[\langle \mathcal{P}^2_{B/W} \rangle - \langle \mathcal{P}_{B/W} \rangle^2] , \tag{2.13}$$

which ought to diverge critically at $T_{B/W}$. In order to monitor the fluctuations in energy at a transition we evaluate the specific heat

$$C_V=\frac{1}{\mathcal{N}}\frac{1}{k_BT^2}[\langle \mathcal{E}^2 \rangle - \langle \mathcal{E} \rangle^2] , \tag{2.14}$$

where $k_B=1$, T is measured in units of J, and $\langle \mathcal{E} \rangle$ is the total average configurational energy.

Thermal roughening of the surface is detected through the behavior of the local height fluctuations

$$\langle \delta h^2 \rangle = \frac{1}{\mathcal{N}} \sum_i \langle [h(\mathbf{r}_i)-\bar{h}]^2 \rangle , \tag{2.15}$$

where $\bar{h}=\sum_i h(\mathbf{r}_i)/\mathcal{N}$ (not necessarily an integer number) is the nominal surface height for a given configuration and the sum is carried out over the lattice sites. This quantity is directly related to the height-height correlation function

$$G(r)=\langle [h(\mathbf{r})-h(\mathbf{0})]^2 \rangle \tag{2.16}$$

(where $r \equiv |\mathbf{r}|$, and the angular brackets denote an ensemble average in the SOS system), which gives a measure of the delocalization of the interface due to fluctuations in height between different regions of the surface. Similarly to $G(r)$, the height fluctuations behave as

$$\langle \delta h^2 \rangle \approx \begin{cases} K(T)\ln(\xi/a), & T<T_R \\ K(T)\ln(L/a), & T \geq T_R \end{cases} , \tag{2.17}$$

thus saturating to a constant value for temperatures below T_R (smooth phase), while logarithmically diverging with the system's linear size $L=Na$ for $T>T_R$, the roughening transition temperature. In order to locate this temperature, we search for the characteristic Kosterlitz-Thouless behavior of $K(T)$ (Ref. 3)

$$K(T)=\begin{cases} \dfrac{1}{\pi^2}, & T=T_R \\ \dfrac{1}{\pi^2}+C(T-T_R)^{1/2}, & T \to T_R^+ \end{cases} , \tag{2.18}$$

where C is a nonuniversal constant, while the value $K(T_R)$ and the power $\frac{1}{2}$ are universal features.

In order to relate the order parameter and its fluctuations to measurable quantities, we also evaluate the total atom scattering intensity from our surface structures within the kinematic approximation. This is given by

$$I(\mathbf{Q},q_z)=\langle \mathcal{I}(\mathbf{Q},q_z) \rangle = \frac{1}{\mathcal{N}^2}\left\langle \left| \sum_i e^{i\mathbf{Q}\cdot\mathbf{r}_i} e^{iq_z h(\mathbf{r}_i)} \alpha(\mathbf{r}_i) \right|^2 \right\rangle , \tag{2.19}$$

where $\mathbf{Q}$ and q_z are the surface parallel and perpendicular momentum transfers, respectively, $\mathbf{r}_i$ runs over the surface atom positions, and $\alpha(\mathbf{r}_i)$ is a shadowing factor, included because atoms surrounding a lower (higher) one make it less (more) visible to the probing atomic beam. A reasonable approximation is[20,31] $\alpha(\mathbf{r}_i)=2-\frac{1}{2}n(\mathbf{R})$, where $n(\mathbf{R})$ is the number of near neighbors of the atom at site $\mathbf{R}$ located at a level higher than the atom itself. It can be demonstrated at this point that Eq. (2.19) with $q_z=(2l+1)\pi/a_z$ (known as antiphase condition, $l=0,\pm1,\pm2,\ldots$) yields the general relation between scattering intensities, order parameters, and their fluctuations:

$$I\left[\mathbf{Q},q_z=\frac{\pi}{a_z}\right] \propto P^2_{B/W}\delta(\mathbf{Q})+\frac{k_BT}{\mathcal{N}}\chi_{B/W}(\mathbf{Q}) , \tag{2.20}$$

where $\chi_{B/W}(\mathbf{Q})$ is the Fourier component of the local order-parameter susceptibility. The two contributions to the scattering intensity appearing in the above expression are known in the literature as the coherent and incoherent term, respectively.

III. A LIMIT CASE: THE BCSOS MODEL

The simplest surface model which is of the SOS type, but does embody the presence of two sublattices, is van Beijeren's well-known BCSOS model.[25] It is mapped onto the F version of the six-vertex model, for which many properties are known exactly. It is therefore of interest to enquire about sublattice disordering within the BCSOS model, also to test our Monte Carlo simulation technique against exact results. We shall see that the study of this limit case of our model also leads to useful insight on the properties of the rough phase of a surface.

In what follows we verify that $P_{B/W}$ (defined in Sec. II) coincides with the Legendre conjugate to Baxter's staggered field in the F model.[32,33] We find that $P_{B/W}$ vanishes continuously at T_R, so that sublattice disordering and roughening coincide in the BCSOS model. For other relevant quantities, such as the sublattice susceptibility, there is no exact expression and we therefore perform a Monte Carlo finite-size scaling study, similar to what will be needed for more realistic systems. The results are very instructive, both for the BCSOS model, where an early conjecture by Baxter is checked, and in establishing a viable method for qualifying separately sublattice disordering and roughening phenomena.

For the F model we define, in the notation of Lieb and Wu[34]

$$\Delta=-\cosh\lambda=\frac{a^2+b^2-c^2}{2ab} , \tag{3.1}$$

with $a=b=\exp(-\epsilon/k_BT)$ and $c=1$ the Boltzmann weights associated with the vertices of the F model. Then the probabilities $p(h)$ and $b(h)$ are known to be[35]

$$p(h)=\text{const}\exp[-\lambda(h-\tfrac{1}{2})^2] \tag{3.2}$$

and[31]

$$b(h)=\begin{cases}\sum_{n=0}^{\infty}(-1)^n\exp[-\lambda n(n+2h-1)] & \text{for } h>0\\ 1-b(-h+1) & \text{for } h\le 0\ .\end{cases} \tag{3.3}$$

$P_{B/W}$ is then defined through Eq. (2.9) when Eqs. (3.2) and (3.3) are used.

An alternative definition of order parameter was given by Baxter for the F model.[32,33] In the notation of Baxter, after partitioning the vertex lattice (dual of the site lattice) in two sublattices A and B, an energy $-s$ ($+s$) is associated to every horizontal (vertical) arrow pointing from an A vertex to a B vertex and $+s$ ($-s$) if it points from B to A. In correspondence with the B and W top layer degeneracy of the site lattice, the vertex ground state is twofold degenerate in the following way: in one configuration all five vertices belong to the A sublattice and all six vertices to the B sublattice; in the other configuration the converse is true. In this way s has the character of a staggered external field and is the equivalent of the magnetic field of the Ising model as is able to lift the degeneracy of the ground state. Thus the order parameter which corresponds to this field is simply

$$P_s=-(\partial f/\partial s)_T\ , \tag{3.4}$$

where f is the free energy per vertex. With the introduction of the field, the F model becomes unsolvable, except for $T=2T_R$.[32] However, the order parameter P_s in zero field is known exactly at all temperatures and is given by[33]

$$P_s(s\to 0^+)=\left[\prod_{n=1}^{\infty}\tanh(n\lambda)\right]^2=\left[1+2\sum_{n=1}^{\infty}(-1)^n\exp(-2n^2\lambda)\right]^2\ . \tag{3.5}$$

It can be shown at this point that the series expansions for $P_{B/W}$ and P_s are identical, so that the two order parameters are taken to be one and the same $P_{B/W}$. The special feature of this quantity is that it vanishes with all its temperature derivatives at the roughening temperature T_R given by

$$k_B T_R=4J/\ln 2\simeq 5.771J\ , \tag{3.6}$$

with $J=\epsilon/4$ the BCSOS coupling constant. This behavior characterizes the sublattice order parameter of the infinite-order roughening transition.

No information is available, however, on the behavior of the staggered field susceptibility, $\chi=-(\partial^2 f/\partial s^2)_T$, except again at $T=2T_R$ and $s\to 0^+$, where it diverges as $\ln s$. Nevertheless, Baxter[33] has proposed that for $s=0$ and in the neighborhood of T_R this susceptibility should obey the scaling ansatz (responsible for the ordinary scaling relation $\alpha+2\beta+\gamma=2$):

$$\chi_{B/W}\sim P_{B/W}^2/f_{\text{sing}}\ , \tag{3.7}$$

where f_{sing} is the singular part of the free energy. If one considers[36] that $f_{\text{sing}}\sim\exp(-\pi^2/\lambda)$ and that

$$P_{B/W}\sim\lambda^{-1}\exp(-\pi^2/4\lambda)\ , \tag{3.8}$$

one arrives at

$$\chi_{B/W}\sim\lambda^{-2}\exp(\pi^2/2\lambda)\ , \tag{3.9}$$

which implies a very strong divergence at T_R, since, near T_R, $\lambda\sim(T_R-T)^{1/2}$.

We now examine the general temperature behavior of both $P_{B/W}$ and $\chi_{B/W}$ by means of Monte Carlo simulation of the BCSOS model. In a finite-size lattice, the operative definition of Eqs. (2.11) and (2.13) is used. In Figs. 4 and 5 we report our Monte Carlo results for the temperature dependence of the specific heat C_V and its first temperature derivative dC_V/dT [evaluated using Eq. (4.2) below] for different linear lattice sizes $N=10$, 16, 20, 24, 28, and 32. We stress the total lack of size dependence in both quantities, to be compared with the critical behavior of dC_V/dT for finite κ (Sec. IV). In Fig. 6 the height fluctuations are plotted as a function of temperature and size; the procedure we adopt for determining T_R is the study of the interfacial width divergence at and above roughening within finite-size scaling.[22] The prefactor $K(T)$ is extracted from the fitting of $\langle\delta h^2\rangle$ as a function of the logarithm of the size; in turn, the quantity $[K(T)-1/\pi^2]^2$ defines T_R as its linearly extrapolated zero, as indicated by Eq. (2.17). As clearly shown by our Monte Carlo data this procedure yields a reasonable estimate of $T_R=5.66\pm0.11$, to be compared with Eq. (3.6).

The order parameter $P_{B/W}$ for different lattice sizes is reported in Fig. 7. The infinite system behavior (also reported for convenience) is approached slowly, like $N^{-1/2}\ln N$ at T_R, as finite-size scaling would suggest. Indeed, from the asymptotic behavior of $P_{B/W}$, Eq. (3.8), and of $\xi\sim\exp(\pi^2/2\lambda)$ for the infinite system correlation length, the saturation of $\xi\sim Na$ in the critical region for a finite but large system implies $\lambda\sim(\pi^2/2)/\ln N$ and therefore $P_{B/W}\sim N^{-1/2}\ln N$.

Having checked the method against exact results, the main purpose of this section consists in reporting novel data for the staggered field susceptibility $\chi_{B/W}$, as shown in Fig. 8. In the infinite system, $\chi_{B/W}$ diverges at T_R remaining infinite above. For a finite lattice, we find a divergence with size typical of infinite-order transitions of

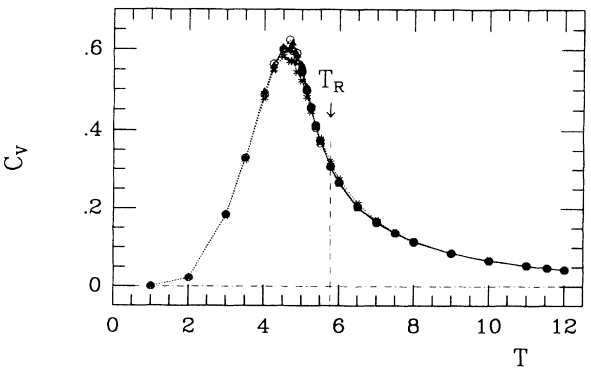

FIG. 4. Specific heat (arbitrary units) vs temperature in the BCSOS model for six system sizes. The arrow indicates the position of the roughening temperature.

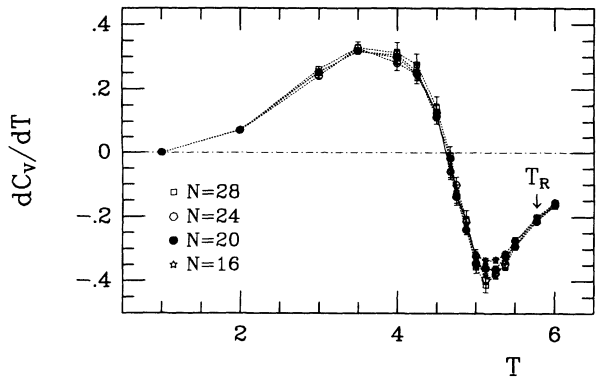

FIG. 5. The first derivative dC_V/dT in the BCSOS model.

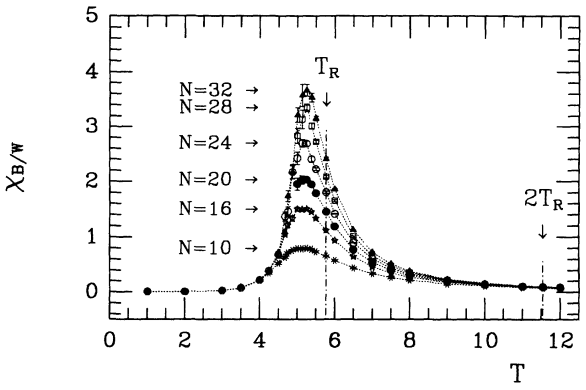

FIG. 8. Staggered field susceptibility (arbitrary units) in the BCSOS model. Notice the markedly different divergence with size at T_R and $2T_R$, respectively.

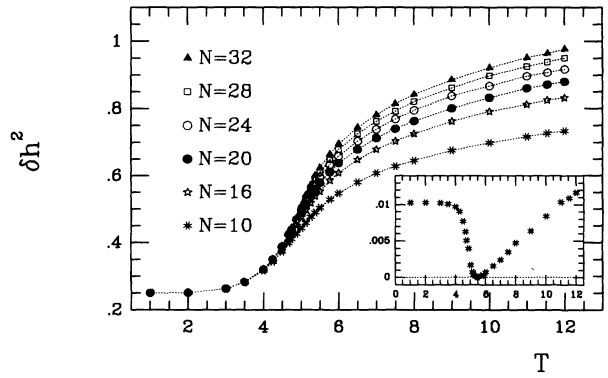

FIG. 6. Finite-size behavior of the average square interfacial width in the BCSOS model. In the inset, the behavior of $[K(T)-1/\pi^2]^2$ is reported in order to determine T_R from extrapolation of the linear temperature dependence (see text).

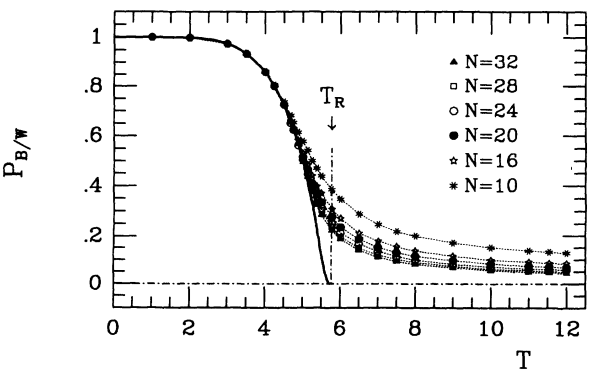

FIG. 7. Sublattice order parameter in the BCSOS model. The solid line represents the infinite system exact behavior.

the form

$$\chi_{B/W}(N,T)\sim N^{\omega(T)} \tag{3.10}$$

with a temperature-dependent new exponent ω. Exactly at T_R, Baxter's ansatz, Eq. (3.7), would imply (barring logarithmic corrections)

$$\omega(T_R)=1\ . \tag{3.11}$$

This follows from the asymptotic form for the correlation length in a finite system near T_R. Our data are compatible with $\omega=1$; we can exploit our knowledge of the infinite system T_R in order to get $\omega(T_R)=0.98\pm0.06$ as obtained from fitting our data for the largest size systems. Furthermore we observe that the peak in $\chi_{B/W}(N,T)$ (which might be taken as a measure of T_R) shifts very slowly towards T_R, like $(\ln N)^{-2}$ to be precise. This follows from $\lambda\sim\sqrt{T_{\rm peak}-T_R}\sim 1/\ln N$. In turn, this whole procedure may represent a way of determining the roughening temperature in models of the BCSOS type where the transition point is unknown. Indeed, $\chi_{B/W}$ is the only sensible diverging quantity in an otherwise smooth phase transition.

We now present for the BCSOS system an exact analysis for the temperature behavior of the new exponent $\omega(T)$ for $T\geq T_R$. Considering the planar six vertex lattice associated, in van Beijeren's mapping,[25] with the lattice of column heights, if the lattice sites are labeled by $\mathbf{R}=(n,m)$, the arrow-arrow correlation function $G_{AA}(R)$ is defined as the thermal average of the product of two arrows separated by a distance $R=|\mathbf{R}|$. Its evaluation in full is difficult; however, when the parameter Δ, Eq. (3.1), vanishes ("free fermion" condition, equivalent to $T=2T_R$ in the F model), its exact evaluation is possible[37] and yields for large $\mathbf{R}$

$$G_{AA}(R)\simeq\frac{2}{\pi^2R^2}\left[\cos\pi(n-m)+\frac{m^2-n^2}{R^2}\right]\ . \tag{3.12}$$

In particular, for two arrows belonging to the same row (i.e., $m=0$, notice, however, that the square arrow lattice is rotated by $\pi/4$ with respect to the atomic lattice) Eq. (3.12) simplifies to

$$G_{AA}(n)\simeq\begin{cases}0 & \text{if } n \text{ even}\\ -\dfrac{4}{\pi^2 n^2} & \text{if } n \text{ odd},\end{cases} \tag{3.13}$$

where it is evident that this arrow-arrow correlation function oscillates from odd to even sites and it decays like R^{-2} at $T=2T_R$. As noted by Youngblood, Axe, and McCoy,[38] the rapidly oscillating contributions decay more slowly than R^{-2} for $T<2T_R$, becoming increasingly important as T_R is approached from above. Ultimately, at $T=T_R$, where the transition to a state of antiferroelectric long-range order of arrows takes place, the discreteness of the lattice becomes essential. For $T\neq 2T_R$ the asymptotic behavior of $G_{AA}(R)$ is known from a calculation employing the quantum inverse scattering method by Bogoliubov, Izergin, and Korepin,[39] which leads to the following generalization of Eq. (3.13):

$$G_{AA}(R)\simeq\frac{K(T)}{n^2}+(-1)^n\frac{K'(T)}{n^{\theta(T)}}, \tag{3.14}$$

valid in the absence of ferroelectric long-range order. It is important to note that the coefficient $K(T)$ is exactly the same as in Eqs. (2.17) and (2.18). The crucial result of Bogoliubov, Izergin, and Korepin is then the following relation between the exponent θ and $K(T)$:

$$\theta(T)=\pi^2 K(T), \tag{3.15}$$

thus confirming the predictions of Youngblood, Axe, and McCoy if the behavior of $K(T)$ from, e.g., Fig. 6, is considered. The staggered susceptibility $\chi_{B/W}$ is related to the arrow-arrow correlation function through the usual fluctuation-dissipation formula

$$\chi_{B/W}=\int_a^{Na} d^2R\, G_{\text{stagg}}(R). \tag{3.16}$$

Here a is the lattice spacing acting as a small distance cutoff, Na is the system's linear size, and a factor $(-1)^n$ is included to give the right staggered character to $\chi_{B/W}$: $G_{\text{stagg}}(n)=(-1)^n G_{AA}(n)$. The equivalent formula valid for the discrete lattice is

$$\chi_{B/W}\sim -K(T)\sum_{n=1}^{N}\frac{(-1)^n}{n}+K'(T)\sum_{n=1}^{N}\frac{1}{n^{\theta(T)-1}} \tag{3.17}$$

and while the first series converges to $A(T)$, the second behaves as $B(T)/N^{\theta(T)-2}$ for $N\gg 1$, with A and B constants. Therefore we have

$$\chi_{B/W}(N,T)\sim A(T)+B(T)N^{\omega(T)}, \tag{3.18}$$

where

$$\omega(T)=2-\theta(T)=2-\pi^2 K(T),\quad T\geq T_R. \tag{3.19}$$

This formula could also be derived from an argument involving scattering functions.[42] The Monte Carlo simulation data are in reasonable agreement with Eq. (3.19); the exponent ω extracted from the raw data for $\chi_{B/W}$ is plotted in Fig. 9, where it is also compared with the quantity $2-\pi^2 K(T)$ extracted from the data for the height fluctuations $\langle \delta h^2\rangle$ of Fig. 6 and with the same quantity obtained from the exact solution of the BCSOS model,

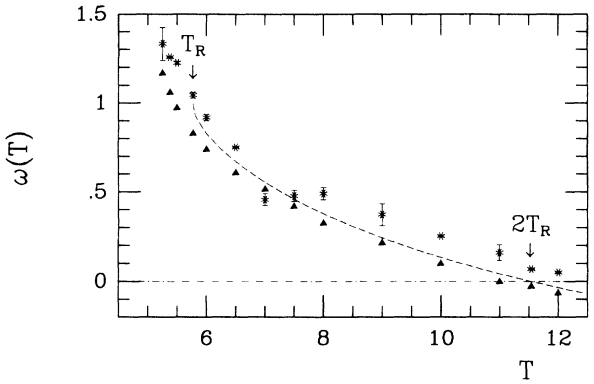

FIG. 9. The exponent ω as a function of temperature. The asterisks are extracted from a fitting of the staggered susceptibility, the triangles are an expression of the formula $\omega(T)=2-\pi^2 K(T)$ [with $K(T)$ from Fig. 5], and the dashed line is obtained from the exact behavior of $K(T)$ [Eq. (3.20)].

$$K(T)=\frac{1}{\pi\arccos\Delta(T)}, \tag{3.20}$$

with Δ defined by Eq. (3.1). We stress that the value $K(T_R)=1/\pi^2$ confirms Baxter's ansatz for $\omega(T_R)=1$. $K(2T_R)=2/\pi^2$ implies a logarithmically weak size dependence of $\chi_{B/W}$ at $2T_R$. This follows from the vanishing of $\omega(T)$ at $2T_R$ or from the usual fluctuation-dissipation formula (3.17) with the form (3.13) for the $G_{AA}(n)$. Finally, the fact that $2/\pi^2<K(T)<3/\pi^2$ for $T>2T_R$ indicates that $\chi_{B/W}$ is no more divergent in this temperature range. This feature is connected to the temperature $T=2T_R$ being known as the "disorder point" for the F model, that is, where the dominant correlations change from an oscillatory to a monotonic behavior. We therefore point out that the divergent behavior of the $\chi_{B/W}$ for a finite system is characteristic only of the temperature interval $[T_R,2T_R]$.

We have shown in this section that sublattice disordering and roughening occur together at $T=T_R$, and with the same Kosterlitz-Thouless behavior, in this model. Our definition of sublattice order parameter and susceptibility, as well as the Monte Carlo finite-size scaling method which allows for a separate study of sublattice disordering and of roughening, can now be taken over to more realistic values of the parameters K_2 and K_3.

IV. THE CASE OF A REAL NONRECONSTRUCTED SURFACE

We now turn our interest to the study of surfaces where roughening and sublattice disordering may take place at different temperatures. We will focus on the parameters J, K_2, and K_3 of Eq. (2.4) with which Hamiltonian (2.1) provides a plausible description of the Ag(110) surface. We stress, however, that we expect that similar features will apply to the structural properties of, e.g., Pb(110), Ni(110), and also Cu(110). As will be shown below, the most important of these features is the occurrence of a non-Ising sublattice disordering phase tran-

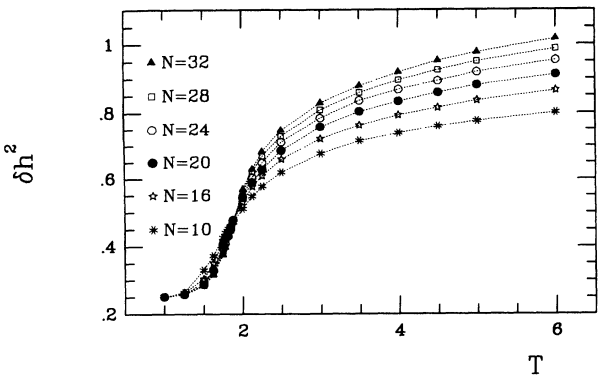

FIG. 10. Temperature and finite-size behavior of the height fluctuations for the Ag(110) Hamiltonian.

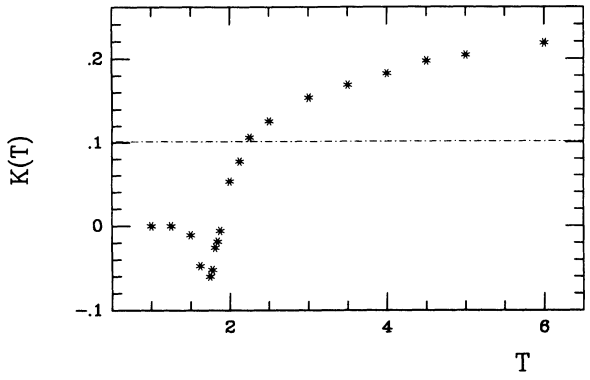

FIG. 12. $K(T)$ plotted as a function of temperature for Ag(110). The dashed line indicates the value $1/\pi^2$.

sition on the flat 1×1 surface before roughening takes place.

We begin by providing evidence for the occurrence of roughening on this model surface. T_R is determined through the usual study of the height fluctuations as function of temperature and system's size. This is presented in Figs. 10–13 and extrapolation of the behavior (2.18) leads to the value

$$T_R = 2.25 \pm 0.07 \ . \tag{4.1}$$

This would correspond to a roughening temperature of ~ 900 K for a cohesion energy parameter $J \simeq 400$ K, in reasonable agreement with the recent measurement of 910 ± 15 K.[7] The linearity of the data for $T > T_R$ in Fig. 13 is remarkable, providing strong evidence for the Kosterlitz-Thouless character of the transition.

We now turn to the search for the in-plane phase transition. As shown in Fig. 14 the peak of the specific heat does not diverge with size N, signaling either an infinite-order transition or a second-order transition with a negative exponent α. Figures 15(a) and 15(b) display the size behavior of dC_V/dT near the peak in C_V, where we have evaluated dC_V/dT from the higher-order combination of the energy cumulants:

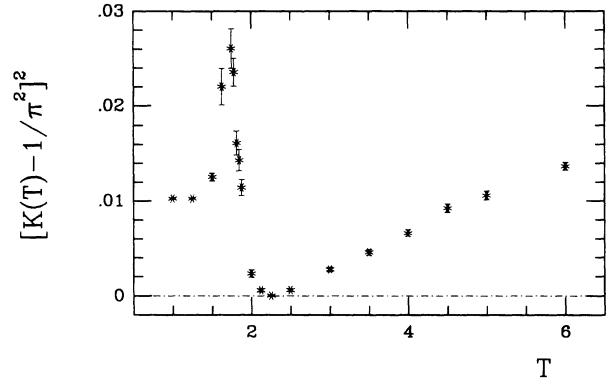

FIG. 13. Plot of the quantity $[K(T)-1/\pi^2]^2$ in order to identify T_R by making use of condition (2.18).

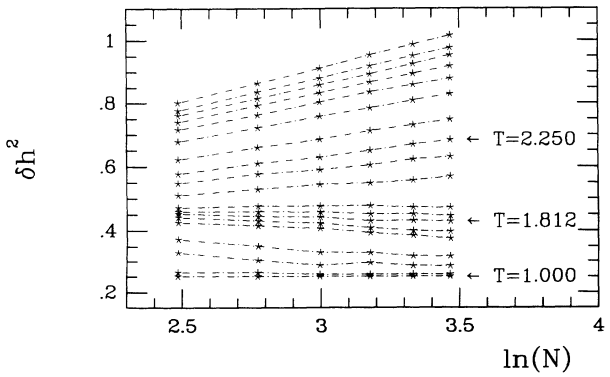

FIG. 11. Size dependence of the height fluctuations plotted in order to extract $K(T)$ for Ag(110). The dependence on $\ln N$ is linear in principle only for $T \geq T_R$.

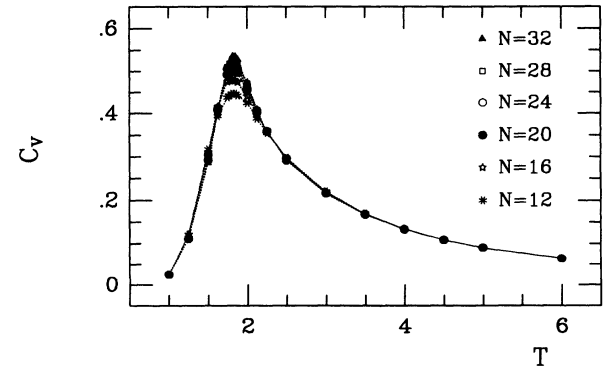

FIG. 14. Specific heat (arbitrary units) vs temperature and the system's size for Ag(110). Notice the absence of a divergent behavior for increasing N.

$$\frac{dC_V}{dT}=\frac{1}{\mathcal{N}}\frac{1}{k_B T^3}\left[-2(\langle \mathcal{E}^2\rangle-\langle \mathcal{E}\rangle^2)+\frac{1}{T}(\langle \mathcal{E}^3\rangle-3\langle \mathcal{E}\rangle\langle \mathcal{E}^2\rangle+2\langle \mathcal{E}\rangle^3)\right] . \tag{4.2}$$

A further temperature derivative of this quantity ought to diverge sharply with an exponent $(\alpha+2)/\nu$ as $N\to\infty$ for a second-order transition. The behavior of dC_V/dT is markedly different from that of the same quantity for the BCSOS model, Fig. 5, and indicates the presence of an ordinary critical point at $T_{B/W}$. This temperature must be extracted from the peak of a sharply divergent quantity such as the sublattice susceptibility. The related order parameter $P_{B/W}$, Eq. (2.11), is presented in Fig. 16. For an infinite system, this parameter should vanish around the disordering temperature (extracted from $\chi_{B/W}$):

$$T_{B/W}=1.81\pm0.03 , \tag{4.3}$$

corresponding to a value of $\sim$750 K, which shows that two distinct phase transitions do occur on this fcc(110) surface, separated by about 20% in temperature. In Fig. 17 we report the behavior of $\chi_{B/W}$, which is now seen to diverge with an exponent $\gamma/\nu>1$. Plotting d^2C_V/dT^2,

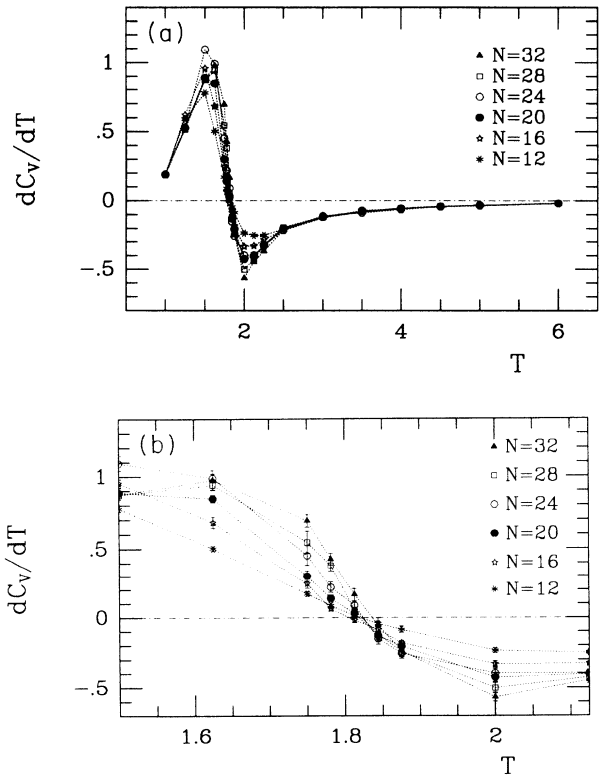

FIG. 15. (a) The first derivative of the specific heat vs temperature for Ag(110). (b) Same as in (a), with an enlarged scale in the critical region, showing the presence of a single critical point.

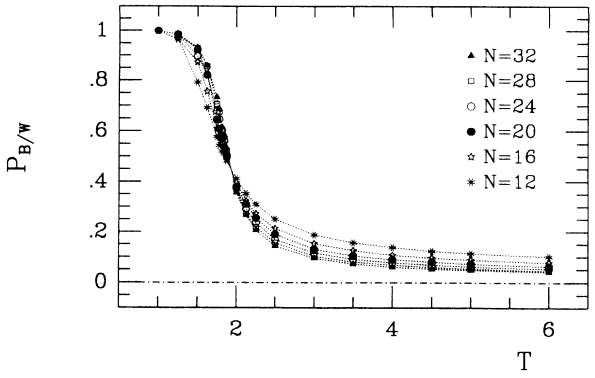

FIG. 16. The sublattice order parameter $P_{B/W}$ for Ag(110).

Fig. 18(a), obtained by numerical differentiation of Eq. (4.2), and the peak of $\chi_{B/W}$, Fig. 18(b), at $T_{B/W}$ versus $\ln N$, we deduce the values

$$\frac{\alpha+2}{\nu}=1.58\pm0.19, \quad \frac{\gamma}{\nu}=1.56\pm0.02 \tag{4.4}$$

from which the exponents

$$\alpha=-0.23\pm0.12, \quad \beta=0.25\pm0.08 , \quad \gamma=1.74\pm0.10, \quad \nu=1.12\pm0.06 \tag{4.5}$$

are estimated, making also use of the scaling relations $\alpha+2\beta+\gamma=2$ and $2-\alpha=d\nu$ $(d=2)$. Within the error bars, the exponents α and β satisfy the extended scaling relation, characterizing preroughening according to den Nijs:[17] $1-\alpha=4\beta$. It should be pointed out that the specific-heat behavior is very different from that of the BCSOS limit case, for which we have no divergence in all temperature derivatives of the free energy. The behavior in the critical region is also very different from that of the Au(110) surface, which fits the exponents of the two dimensional Ising model.[4,12,22] In particular, the exponent β appears to be twice the value characterizing reconstructed surfaces,[4,12,14] a fact with obviously important experimental implications.

We stress that this is the first time, to the authors' knowledge, that a preroughening like transition is predict-

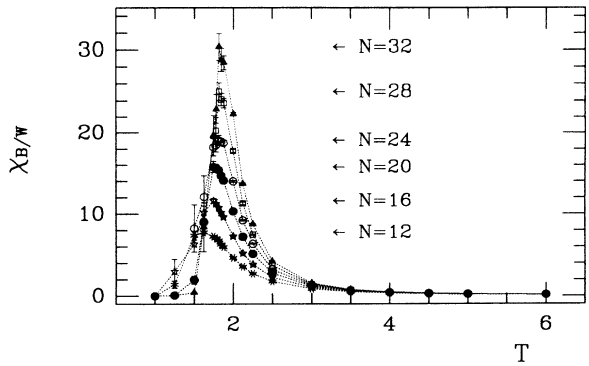

FIG. 17. The sublattice susceptibility $\chi_{B/W}$ (arbitrary units) for Ag(110).

ed with some accuracy in the expected exponents for a particular metal surface, though most of the qualitative features of this study were anticipated by den Nijs.[17] We explicitly confirm the presence of a phase transition on Ag(110), and similar nonreconstructed surfaces, with strongly non-Ising exponents. For all other finite values of $\kappa = K_2/K_3 < 0$ we expect two distinct transitions for these fcc(110) surfaces together with variable critical exponents for the sublattice disordering transition.[16,21]

In order to reveal the nature of the structural phases on our model surface, we turn to the study of the surface scattering intensities, typically considered as a key experimental tool for the investigation of surfaces. One could, in particular, look at the atom scattering intensity given by Eqs. (2.19) and (2.20) through which information on the order parameter and its susceptibility can be obtained. We stress that the antiphase condition is particularly adapted to detect disordering phenomena involving the sublattices of the first two surface layers. From Eq. (2.20) we expect that the height of the antiphase Bragg peak should vanish with a new exponent $2\beta \simeq 0.5$ for nonreconstructed surfaces such as Ag(110). Our simulation for the integer peak scattering intensity is in qualitative agreement with the above picture, with the coherent peak height behaving like $P^2_{B/W}$. Figure 19 shows the incoherent atom scattering pattern calculated for the largest system available ($N=32$), for $Q_y=0$, $q_z=\pi/a_z$, and Q_x in the whole range of investigation, for $T=1.875$, intermediate between $T_{B/W}$ and T_R. The total scattering

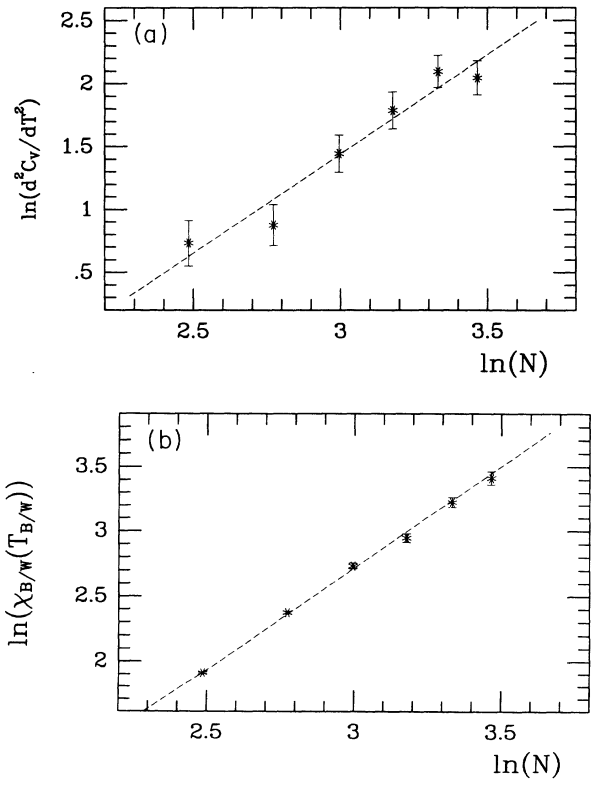

FIG. 18. (a) Scaling of d^2C_V/dT^2 (proportional to the second derivative of the specific heat) at $T_{B/W}$ for Ag(110). (b) Scaling of the susceptibility peak height.

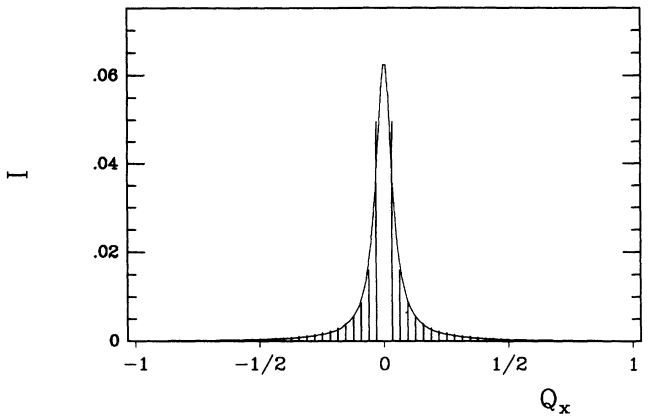

FIG. 19. Incoherent atom scattering pattern (arbitrary units) for the specular peak in antiphase, fitted with a Lorentzian function, for Ag(110). The coherent part at $Q_x=0$ is not reported since it is out of scale. Here and in the following figures $N=32$.

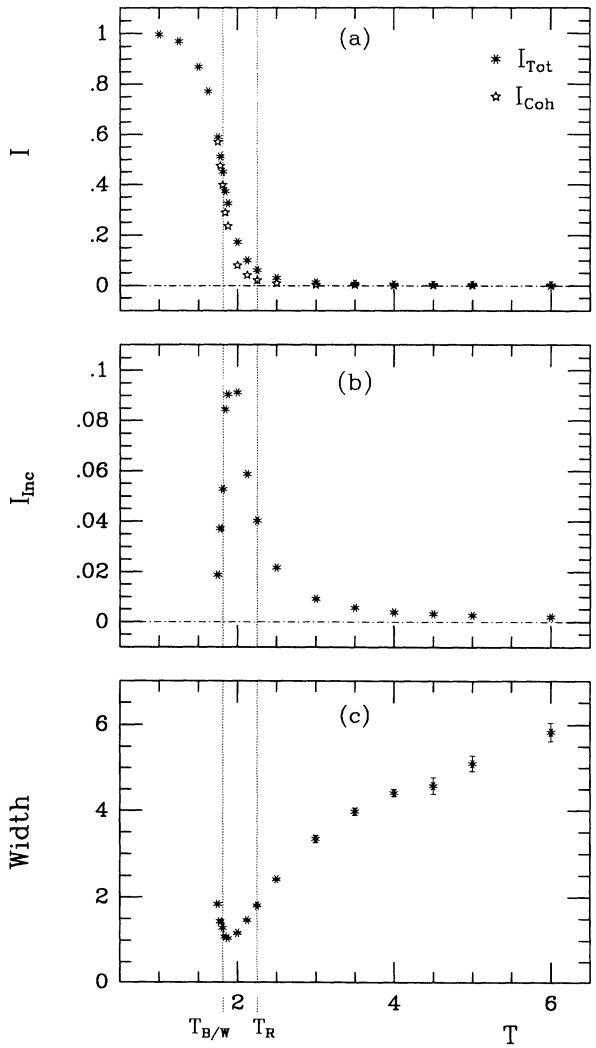

FIG. 20. Temperature dependence of (a) the total and the coherent part of the specular peak in antiphase $(0,0,\pi/a_z)$, (b) the incoherent contribution, and (c) the incoherent peak width for Ag(110). The vertical axis in (b) and (c) is marked in units of $2\pi/Na = 0.048$ Å^{-1}.

intensity, Eq. (2.20), has been evaluated for all temperatures. A fitting of the incoherent part with a Lorentzian function is performed on the data in order to obtain the incoherent peak intensity in antiphase as a function of temperature. Also the coherent peak intensity is obtained by subtraction from the total intensity; all these are reported in Figs. 20(a) and 20(b), together with the incoherent peak width, given in Fig. 20(c). While these intensities give a measure of $P_{B/W}$ and $\chi_{B/W}$, the peak width is a measure of the inverse of the in-plane correlation length ξ. This width shows a drastic increase above $T_{B/W}$, signaling the appearance of steplike defects on the surface. Notice that there is a minimum value for the peak width, expected to vanish at $T_{B/W}$, owing to the usual finite-size restrictions. Finally, contrary to the case of reconstructed Au(110),[22] there is no shift in the incoherent peak position above the in-plane disordering temperature.

V. DISCUSSION AND CONCLUSIONS

The situation studied in Sec. IV, that of the two-stage disordering of a nonreconstructed surface, corresponds to a relatively simple surface disordering scenario. Figure 21 presents snapshots of typical surface configurations as generated by our Monte Carlo simulation of Hamiltonian (2.1) [with (2.4)] for temperatures characterizing the three different structural phases: (a) ordered flat, (b) disordered flat, and (c) rough phases. As an educated inspection of the configurations of Fig. 21 would suggest, steps are the source of both in-plane and off-plane disordering. For $T < T_{B/W}$ only isolated local defects are found on an otherwise flat (110) surface. Their density increases as a function of temperature and compact domain walls (bound pairs of up and down steps) start to appear. None of these cause preroughening, which is instead driven by steps with a long range up-down order. Figure 21(b) might represent such situation on a small scale. This structure is stabilized (as shown by den Nijs[17]) by the positive value of the next-near-neighbor coupling K_3, which acts as an effective hard-core repulsion between two up-up or down-down monoatomic steps. The appearance of these steps is also an explanation for the absence of the shift in the specular peak position, Fig. 19. Two such steps are in fact sufficient to cause the vanishing of $P_{B/W}$ on a finite system, but of course this is not enough to induce a shift which is instead driven by a global increase of the lattice spacing in the x direction. This would arise from the proliferation of, e.g., 2×1 compact domain walls, but this is clearly not the case in a model of Ag(110) displaying the DOF phase. By a further rise in the temperature, the DOF structure evolves into the usual rough phase with a delocalized interface, Fig. 21(c).

The case of a reconstructing fcc(110) surface, such as

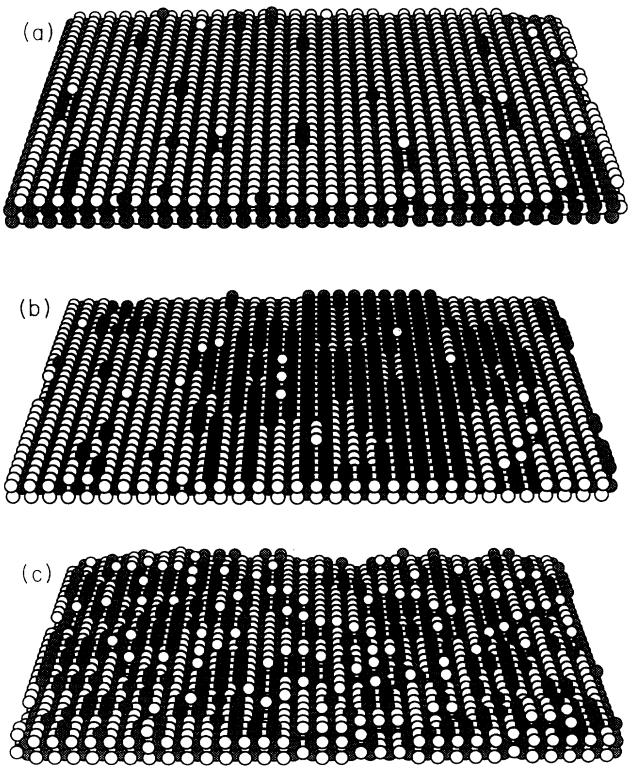

FIG. 21. Snapshots of the surface configuration of Ag(110) as generated by our model and Monte Carlo simulation. (a) $T=1.75$ (below $T_{B/W}$, ordered flat phase), (b) $T=2.00$ (between $T_{B/W}$ and T_R, DOF phase), and (c) $T=6.00$ (above T_R, rough phase). Black and white circles refer to Ag atoms belonging to the two distinct sublattices of the fcc(110) structure. The figure refers to the largest system size ($N=32$); atoms are added below the surface to help visualization of the configuration, though our simulation generates only the surface layer.

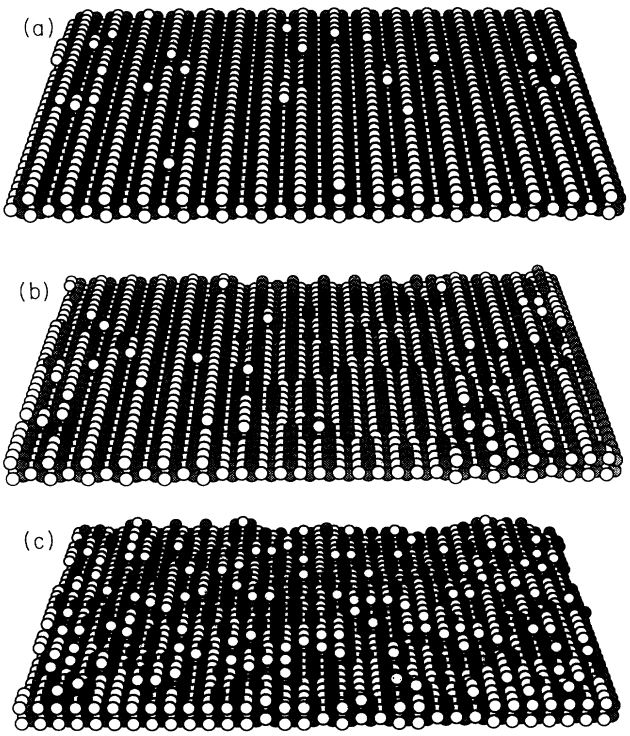

FIG. 22. Snapshots of the surface configuration of Au(110) as generated by our model and Monte Carlo simulation. (a) $T=2.812$ (below T_D, 2×1 reconstructed phase), (b) $T=2.937$ (between T_D and T_R, DOF phase), and (c) $T=8.000$ (above T_R, rough phase).

Au(110), is potentially richer in its disordering scenario, although the intermediate phase temperature window is too narrow to afford a deeper investigation of the disordering processes. In Fig. 22 we present the analogous sequence of snapshots of the Monte Carlo simulation of Au(110) for model (2.1) with the appropriate parameters.[22] The discussion on order parameters presented in Sec. II can be repeated for the reconstructed ground-state surfaces. However, (i) there is a further order parameter $P_{2\times1}$ on these systems (see Ref. 22) which distinguishes the 2×1 ordered phase of Fig. 22(a) from the deconstructed phase of Fig. 22(b) and (ii) there is in principle no reason why this order parameter should vanish at $T_{B/W}$. Indeed, as remarked by Bernasconi and Tosatti,[40] the $P_{2\times1}$ order parameter may vanish before $P_{B/W}$ owing to the proliferation of tightly bound 3×1 up-down pairs of steps which do not lead to a sublattice disordered phase. The resulting structure, which would exist (if at all) between T_D and $T_{B/W}$, would consist of large terraces characterized by reconstructed 2×1 order and the predominance of a specific sublattice in the topmost layer. Above $T_{B/W}$, but still below T_R, $P_{B/W}$ would vanish initially into the DOF phase of den Nijs. With the available data within our simulation[22] we must conclude that T_D and $T_{B/W}$ coincide in our model (2.1) for Au(110). It is not excluded, however, that for some fcc(110) surface the disordering process may consist of three, rather than two, distinct stages.[40] Finally, we point out that for the reconstructed surfaces we are also able to define a preroughening order parameter as the average of a local variable sensitive to a monoatomic step which can also be shown to coincide with the sublattice disordering parameter defined in Ref. 22 (see the Appendix). Therefore, also for reconstructed fcc(110) surfaces we have $T_{B/W}=T_{PR}$.

In conclusion, we have simulated the statistical mechanics of a model of nonreconstructed fcc(110) surfaces. Two separate transitions are found: a sublattice disordering (preroughening) and a standard roughening transition, well separated in temperature and with strongly non-Ising exponents for the specifically studied case of Ag(110). We have described the interesting properties of the intermediate DOF phase and shown that this will disappear, with $T_{B/W}$ and T_R coinciding, in the BCSOS limit when long-range interactions are absent. The DOF phase is generated by the presence of further-neighbor couplings, such as K_3J, on top of the interactions of the BCSOS Hamiltonian. We thus believe that for all finite values of κ the phase diagram will consist of two separate transitions.

As for the experimental situation, we point out that existing experimental data on Ag(110) (Ref. 7) as well as on Ni(110) (Ref. 41) present the common feature of a "knee" in the temperature dependence of the antiphase peak intensity around a temperature that, for Ag(110), is of the same order as our estimated $T_{B/W}$. Further studies are clearly needed to clarify the situation. Indirect evidence for preroughening of Pb(110) at 360 K is provided by high-resolution electron-energy-loss spectroscopy data of Yang *et al.*[15] There is a smooth drop of the antiphase peak intensity, well below the roughening transition independently placed at 415 ± 10 K. Such a smooth drop is compatible with a large value of the exponent β, as found in this work. However, this evidence is also not definitive because of an apparent anisotropy of antiphase scattering, which is thus far unexplained. In summary, hitherto no clear experiment has yet revealed the transition at $T_{B/W}$ and we hope that our work may stimulate further experimental research on nonreconstructed fcc(110) or other crystal surfaces with a two-sublattice structure.

APPENDIX

We sketch the demonstration that, for 2×1 reconstructed fcc(110) surfaces, the appropriate sublattice order parameter is identical to a suitably defined preroughening order parameter sensitive to the occurrence of monoatomic steps on the flat surface. The proof proceeds along the lines of that given in Sec. II for the nonreconstructed case.

Define the local spin variable, for, e.g., a B site atom

$$S_i^B=\tfrac{1}{4}\sum_{\delta}[h(\mathbf{r}_i)-h(\mathbf{r}_i+\delta)] \tag{A1}$$

taking values $+1$, 0, and -1 ($\frac{1}{2}$ and $-\frac{1}{2}$, always present, get coarsened away) according to whether the B atom is on top, in the middle of the (111) microfacet, or at the bottom of the 2×1 groove. The analogous quantity S_i^W is defined for a W atom at site $\mathbf{r}_i$. Then, the sublattice order parameter is

$$P_{B/W}=\frac{1}{2\mathcal{N}}\left\langle\sum_{i\in W}|S_i^W|-\sum_{i\in B}|S_i^B|\right\rangle , \tag{A2}$$

which, as it should, takes values $+1$ (-1) when all W (B) atoms occupy the topmost layer and 0 when the symmetry between the W and B sublattices is restored.

Now, consider the following local preroughening variables:

$$\sigma_i=\begin{cases}2|S_i^B|-1 & \text{if } i\in B\\ 1-2|S_i^W| & \text{if } i\in W\end{cases} . \tag{A3}$$

This takes values ±1 (when coarsened), changing sign every time a step is encountered on a 2×1 flat terrace, independently of the sublattice type. Hence

$$\rho=\langle\sigma_i\rangle \tag{A4}$$

is the appropriate preroughening order parameter. We can express it in a global representation through

$$\rho=\frac{1}{\mathcal{N}}\left\langle\sum_i\sigma_i\right\rangle=P_{B/W} , \tag{A5}$$

so that again it coincides with the sublattice order parameter.

*Also at International Centre for Theoretical Physics, Strada Costiera 11, 34014 Trieste, Italy.

[1]E. Bauer, in *Structure and Dynamics of Surfaces II,* edited by W. Schommers and P. Von Blanckenhagen (Springer, Heidelberg, 1987).

[2]R. F. Willis, in *Dynamical Phenomena at Surfaces, Interfaces and Superlattices,* edited by F. Nizzoli, K. H. Rieder, and R. F. Willis (Springer, Berlin, 1985).

[3]H. van Beijeren and I. Nolden, in *Structure and Dynamics of Surfaces II* (Ref. 1).

[4]J. C. Campuzano, M. S. Foster, G. Jennings, R. F. Willis, and W. Unertl, Phys. Rev. Lett. **54**, 2684 (1985).

[5]G. A. Held, J. L. Jordan-Sweet, P. M. Horn, A. Mak, and R. Birgeneau, Phys. Rev. Lett. **59**, 2075 (1987).

[6]I. K. Robinson, E. Vlieg, H. Hornis, and E. H. Conrad, Phys. Rev. Lett. **67**, 1890 (1991).

[7]G. Bracco, C. Maló, C. J. Moses, and R. Tatarek, Surf. Sci. **287/88**, 871 (1993).

[8]H.-N. Yang, T.-M. Lu, and G.-C. Wang, Phys. Rev. Lett. **63**, 1621 (1989).

[9]P. Zeppenfeld, K. Kern, R. David, and G. Comsa, Phys. Rev. Lett. **62**, 63 (1989).

[10]J. Sprösser, B. Salanon, and J. Lapujoulade, Europhys. Lett. **16**, 283 (1991).

[11]M. Krzyzowsky and K. Kern (private communication).

[12]D. T. Keane, P. A. Bancel, J. L. Jordan-Sweet, G. A. Held, A. Mak, and R. J. Birgeneau, Surf. Sci. **250**, 8 (1991).

[13]D. Cvetko, A. Lausi, A. Morgante, F. Tommasini, and K. C. Prince, Surf. Sci. **269/270**, 68 (1992).

[14]I. K. Robinson, E. Vlieg, and K. Kern, Phys. Rev. Lett. **63**, 2578 (1989); **65**, 1831 (1990).

[15]H.-N. Yang, K. Fang, G.-C. Wang, and T.-M. Lu, Europhys. Lett. **19**, 215 (1992).

[16]K. Rommelse and M. den Nijs, Phys. Rev. Lett. **59**, 2578 (1987); M. den Nijs and K. Rommelse, Phys. Rev. B **40**, 4709 (1987).

[17]M. den Nijs, Phys. Rev. Lett. **64**, 435 (1990); **66**, 907 (1991); Phys. Rev. B **46**, 10 386 (1992).

[18]J. Villain and I. Vilfan, Phys. Rev. Lett. **65**, 1830 (1990); Surf. Sci. **257**, 368 (1991).

[19]L. Balents and M. Kardar, Phys. Rev. B **46**, 16 031 (1992).

[20]A. Trayanov, A. C. Levi, and E. Tosatti, Surf. Sci. **233**, 184 (1990).

[21]J. Kohanoff, G. Jug, and E. Tosatti, J. Phys. A **23**, L209 (1990); **23**, 5625 (1990).

[22]G. Mazzeo, G. Jug, A. C. Levi, and E. Tosatti, Surf. Sci. **273**, 237 (1992).

[23]G. Mazzeo, G. Jug, A. C. Levi, and E. Tosatti, J. Phys. A **25**, L967 (1992).

[24]G. Mazzeo, G. Jug, A. C. Levi, and E. Tosatti, Europhys. Lett. **22**, 39 (1993).

[25]H. van Beijeren, Phys. Rev. Lett. **38**, 993 (1977).

[26]S. P. Chen and A. F. Voter, Surf. Sci. **244**, L107 (1991).

[27]F. Ercolessi, A. Bartolini, M. Garofalo, M. Parrinello, and E. Tosatti, Phys. Scr. **19**, 399 (1987).

[28]A. C. Levi and M. Touzani, Surf. Sci. **218**, 223 (1989).

[29]C. Jayprakash and W. F. Saam, Phys. Rev. B **30**, 3916 (1984).

[30]G. E. Tommei, A. C. Levi, and R. Spadacini, Surf. Sci. **125**, 312 (1982).

[31]A. C. Levi, R. Spadacini, and G. E. Tommei, in *The Structure of Surfaces II,* edited by J. F. van der Veen and M. A. van Hove (Springer, Berlin, 1988), Vol. 11.

[32]R. J. Baxter, Phys. Rev. B **1**, 2199 (1970).

[33]R. J. Baxter, J. Phys. C **6**, L94 (1973).

[34]E. H. Lieb and F. Y. Wu, in *Phase Transitions and Critical Phenomena,* edited by C. Domb and M. S. Green (Academic, London, 1972), Vol. 1.

[35]P. J. Forrester, J. Phys. A **19**, L143 (1986).

[36]R. J. Baxter, *Exactly Solvable Models in Statistical Physics* (Academic, London, 1982).

[37]B. Sutherland, Phys. Lett. **26A**, 532 (1968).

[38]R. W. Youngblood, J. D. Axe, and B. M. McCoy, Phys. Rev. B **21**, 5212 (1980).

[39]N. M. Bogoliubov, A. G. Izergin, and V. E. Korepin, Nucl. Phys. B **275**, 687 (1986), and references therein.

[40]M. Bernasconi and E. Tosatti, Surf. Sci. Rep. **17**, 363 (1993).

[41]Y. Cao and E. H. Conrad, Phys. Rev. Lett. **64**, 447 (1990).

[42]L.-H. Tang (private communication).

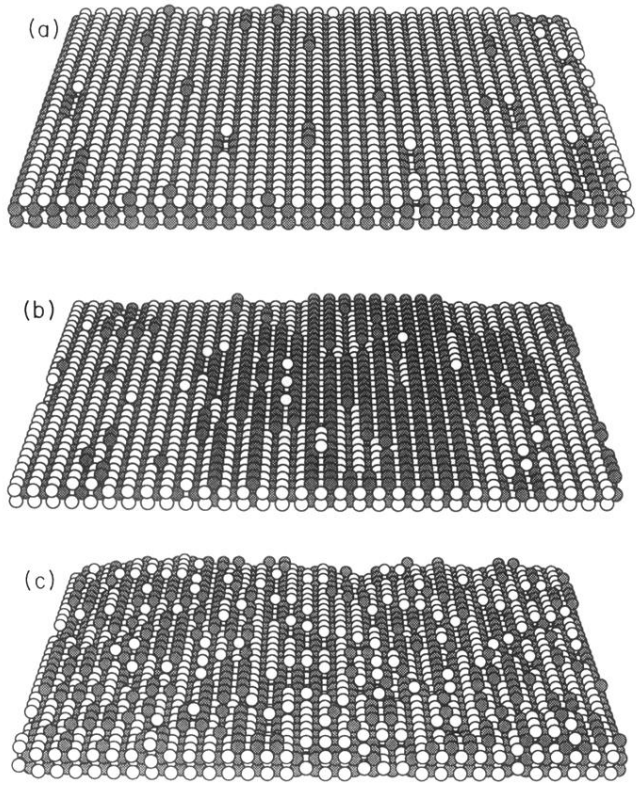

FIG. 21. Snapshots of the surface configuration of Ag(110) as generated by our model and Monte Carlo simulation. (a) $T=1.75$ (below $T_{B/W}$, ordered flat phase), (b) $T=2.00$ (between $T_{B/W}$ and T_R, DOF phase), and (c) $T=6.00$ (above T_R, rough phase). Black and white circles refer to Ag atoms belonging to the two distinct sublattices of the fcc(110) structure. The figure refers to the largest system size ($N=32$); atoms are added below the surface to help visualization of the configuration, though our simulation generates only the surface layer.

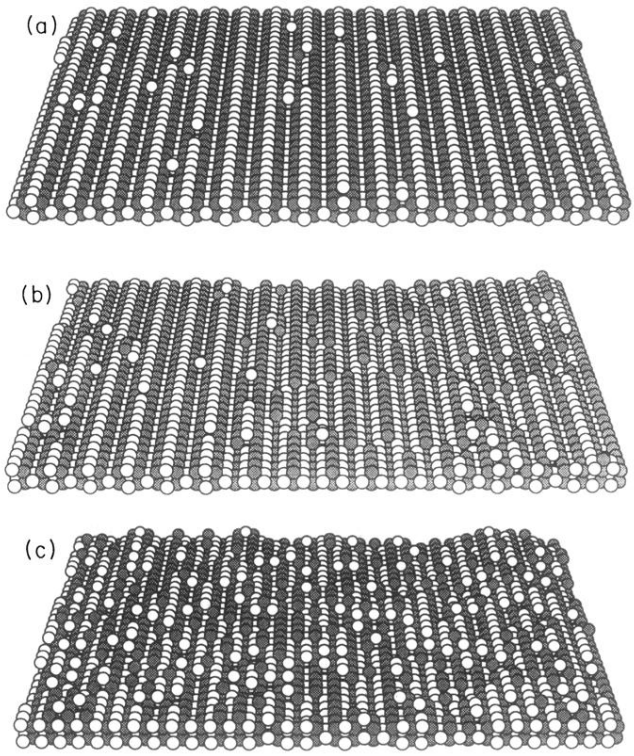

FIG. 22. Snapshots of the surface configuration of Au(110) as generated by our model and Monte Carlo simulation. (a) $T=2.812$ (below T_D, 2×1 reconstructed phase), (b) $T=2.937$ (between T_D and T_R, DOF phase), and (c) $T=8.000$ (above T_R, rough phase).